

Investigation of static and dynamic mechanical loads on light-weight PV modules for offshore floating applications

Peer-reviewed author version

KYRANAKI, Nikoleta; NIVELLE, Philippe; BOUGUERRA, Sara; CASASOLA PAESA, Marta; DE JONG, Richard; Delbeke, Oscar; Spannan, Lars; VAN DER HEIDE, Arvid; KAAYA, Ismail; Moschner, Jens; MORLIER, Arnaud & DAENEN, Michael (2024) Investigation of static and dynamic mechanical loads on light-weight PV modules for offshore floating applications. In: Engineering structures, 319 (Art N° 118760).

DOI: 10.1016/j.engstruct.2024.118760

Handle: <http://hdl.handle.net/1942/44280>

Investigation of Static and Dynamic Mechanical Loads on Light-Weight PV Modules for Offshore Floating Applications

Nikoleta Kyranaki^{*a,b,c}, Philippe Nivelles^{a,b,c}, Sara Bouguerra^{a,b,c}, Marta Casasola Paesa^{a,b,c}, Richard De Jong^{a,b,c}, Oscar Delbeke^{c,d}, Lars Spannan^e, Arvid van der Heide^{a,b,c}, Ismail Kaaya^{a,b,c}, Jens Moschner^{c,d}, Arnaud Morlier^{a,b,c}, Michaël Daenen^{a,b,c}

^a Institute for Materials Research (IMO), Hasselt University, Diepenbeek, Belgium

^b Imec, Imo-Imomec, Thor Park, Genk, Belgium

^c EnergyVille, Genk, Belgium

^d KU Leuven, ESAT-ELECTA, Leuven, Belgium

^e KU Leuven, Department of Civil Engineering, Leuven, Belgium

Philippe.nivelles@uhasselt.be, sara.bouguerra@uhasselt.be,
marta.casasolapaesa@uhasselt.be, richard.dejong@imec.be, oscar.delbeke@kuleuven.be,
lars.spannan@kuleuven.be, arvid.vanderheide@imec.be, Ismail.Kaaya@imec.be,
jens.moschner@kuleuven.be, Arnaud.Morlier@imec.be, michael.daenen@uhasselt.be

Corresponding author: Nikoleta Kyranaki

Address: Institute for Materials Research (IMO), Hasselt University, Diepenbeek, Belgium

Imec, Imo-Imomec, Thor Park, Genk, Belgium

EnergyVille, Genk, Belgium

e-mail address: nikoleta.kyranaki@uhasselt.be

Keywords: Floating Photovoltaics, robustness, sustainability, mechanical load, wind, vibrations

Abstract

Photovoltaic (PV) systems are significant for the transition towards renewable energy. However, their expansion is constrained by the scarcity of suitable land in proximity to electric grids. To address this issue, floating PV is a promising solution. Ensuring the robustness of floating PV installations remains a major concern, particularly regarding the mechanical load due to strong winds in open water. This study aims to assess the impact of wind on floating PV modules, by considering real wind speed values occurring at the North Sea. To achieve this objective, the influence of PV module configuration, such as inclination, is examined. Moreover, different thicknesses of PV glass are considered to find an optimum between mechanical stability and material consumption. Lastly, a resonance vibration test is performed and compared to simulations to estimate the effects of vibration on PV module stress. The findings indicate that a low inclination installation is preferable, and a glass-glass PV module with a 2.5 mm glass thickness can withstand static and dynamic mechanical loads, although long-term durability requires further investigation. Additionally, it is crucial for the standard Dynamic Mechanical Load (DML) test to include higher pressure values and an extended vibration test at the resonance frequency with the highest measured acceleration, identified after a frequency sweep.

1. Introduction

With the growing energy demand and the scarcity of traditional energy sources, there is an increasing need for renewable energy. Photovoltaic (PV) generation systems play a significant role in the expansion of renewable energy, with a global cumulative capacity of approximately ~1555 GW (end of 2023) [1]. Solar energy accounted for 4.57% of global electricity generation in 2022 [2], making it the third largest renewable electricity technology after hydropower and wind [3]. However, the availability of suitable land poses a limitation to further growth [4]. Floating PV presents an appealing solution to overcome this constraint by utilizing unused water reservoirs for installations and expanding the potential capacity for renewables.

Floating PV offers numerous advantages, including the avoidance of land usage, enhanced efficiency of PV modules due to reduced thermal impact, minimal shading thanks to a more open area, decreased evaporation loss, diverse application possibilities such as combining it with fish farming, and a promising market potential [5]. The grid connection can be co-utilized with turbines in case of reservoirs, or with wind turbines in offshore use [6,7]. This is primarily because there is a large availability of water bodies suitable for deploying floating PV systems. However, the robustness of such installations necessitates further investigation, as they are susceptible to mechanical loads caused by high wind and wave movements [8], increased moisture ingress [9], salt presence [10], and bio-fouling [5], impacts which are aggravated offshore and they are not sufficiently researched. This study will specifically focus on examining the impact of mechanical loads, as there have already been incidents indicating their detrimental effects on floating PV installations [11].

The scientific innovation of the presented work is that mechanical simulations for both static and dynamic load are included and compared to dynamic mechanical load testing. In literature, either the static [12–14] or dynamic loads [15–17] are studied, but no attention is given to their

respective contribution in the overall reliability of PV modules exposed to real outdoor conditions, including high wind gusts. Moreover, there is only a small number of publications correlating the deformation due to wind loading and the internal stress levels generated as a consequence, and those studies are not looking into high wind gusts, east-west configurations and different glass thicknesses were not considered [14]. This research attempts for the first time according to our knowledge to simplify the estimation of the developed internal stress, caused by multiple sequential wind speeds included within a wind gust, by minimizing the lengthy and computationally expensive Finite Element Method (FEM) simulations. Another important outcome of this study is the comparison of the first principal stress that a PV module would develop when in resonance with this caused by the standard IEC TS 62782:2016 for Dynamic Mechanical Load (DML) testing. Furthermore, we demonstrate the possibility of achieving cost savings by reducing the thickness of the glass used in PV modules. This reduction in glass thickness is particularly important since the cost of glass constitutes approximately 10-25% of the total cost of a PV module [18]. Additionally, by reducing the thickness of the glass, the weight of the modules is also reduced, which is crucial for the installation and Operation and Maintenance (O&M) of a floating PV plant. Finally, this leads to resource conservation through the reduced utilization of glass, thereby contributing to the overall sustainability of the technology.

The aim of this work is to evaluate and compare the static and dynamic mechanical load that a PV module encounters due to strong wind gusts, when installed on an offshore PV platform, and their impact on the stress developed within a PV module. In order to achieve this goal, the effect of configuration of the PV modules (inclination) is examined for a wind speed of 45 m s^{-1} . This value was recorded as the highest gust at the Belgian North Sea (Westhinder) within a period of 7 years (from 2015 to 2022). The highest reported value in Belgium is 55 m s^{-1} in the Lothar Storm in 1999, however, it was not used as it was assumed a very extreme condition. Additionally, the thickness of the glass of the PV module was varied, for the identification of the minimum requirements. Furthermore, a resonance vibration test is carried out and compared to simulations, in order to estimate the influence of the vibration mode with the highest impact on the stresses developed. Finally, the maximum first principal stress and deformation occurring for a PV laminate, due to wind speed variation, was calculated for various wind speeds. The combination of the results contributed to the assessment of the adequacy of the existing standard IEC TS 62782:2016 for DML testing.

2. Experimental Section/Methods

For the investigation of the mechanical loads (static and dynamic) that a PV module may encounter due to wind when installed offshore, a combination of experiments and simulations were utilized. The computation of the pressure distributions, applied on the PV modules by the wind, and the estimation of the first principal stress maps on the top and rear sides of glass-glass PV modules were conducted by FEM simulations with COMSOL Multiphysics. The tilt angle of the PV modules for all the simulations was defined according to the simulation scenario and is reported at each subsection. In the case of dynamic mechanical load and for the identification of the resonance frequencies, a frequency sweep / vibration experiment was realized. The methodology for all the theoretical calculations and the experimental work are described in the following sections.

2.1 Vibration Experiment / Frequency Sweeps

In order to identify the resonance frequencies of the studied PV module, a vibration experiment including frequency sweeps was carried out. A glass-glass n-type bifacial mc-Si PV module (see specifications in **Table 1**) with dimensions 1690 mm x 996 mm x 30 mm (frame thickness), containing 120 (6 x 20) half cells of dimensions 158.75 mm x 79.375 mm and glass of thickness equal to 2.5 mm, was mounted on a vibration table as shown in **Figure 1**. Two aluminum profiles were rigidly attached to the table and the PV module was clamped at four points, according to the number of the aluminum profiles, the dimensions of the PV module and the positioning on the vibration table. Two frequency sweeps were applied, one starting from 3 Hz and finishing at 250 Hz and a reverse. It must be noted that the values obtained below 10 Hz are questionable, due to the inadequate control of the table. More specifically, during the ascending sweep, the table could not start vibrating below 6 Hz, while during the descending sweep, the table continued vibrating until reaching 3 Hz. The acceleration applied by the table was 1 g (see **Figure S1** for the details of the sweep). The acceleration of the PV modules was recorded by an accelerometer ADXL345 of range ± 16 g and resolution 1 msec. The accelerometer was attached to the center of the PV module. The experiment was repeated for two PV modules of the same type, in order to ensure repeatability.

Table 1. Electrical properties of tested PV modules at Standard Test Conditions (STC).

Peak Power (Pmax) (W)	340
MPP Voltage (Vmp) (V)	35.1
MPP Current (Imp) (A)	9.70
Open Circuit Voltage (Voc) (V)	41.8
Short Circuit Current (Isc) (A)	10.17
Module Efficiency (%)	20.20



Figure 1. PV module fixed on the vibration table with aluminum profiles-supports. The exact position of the clamps is indicated.

2.2 FEM Simulations

2.2.1 Mechanical Load (Pressure) due to Wind

The inhomogeneous mechanical load due to wind (pressure in Pa) was estimated as a consequence of a 2D turbulent air flow. For the simulation of the wind flow, the “*Turbulent Flow*” module was used. The “*Geometry*” included a rectangle of width equal to 6 m and height of 10 m. The right side of the rectangle was assumed as the “*Inlet*”, the left side as the “*Outlet*”, the bottom as a “*Wall*” and the top as an “*Open Boundary*” (**Figure 2a**). The bottom “*Wall*” was considered static, as for this study, the floating structure is assumed large and rigid, meaning that the movement due to waves is not significant. The wind velocity of the “*Inlet*” was varied according to the simulation from 5 to 45 m s⁻¹. The value was constant along the inlet, since it was assumed equal to what was measured for the respective height of installation. The “*Turbulence*” model applied was k-ε with a compressible flow (Ma < 0.3) due to its good convergence rate, low memory requirements and accuracy for external flow problems [19]. In order to estimate the pressure variations due to the presence of a PV module, a 2D cross-section was placed at the center of the bottom wall with dimensions 0.01 m width (approximation between the thickness of the frame and the PV laminate) and 0.996 m height, assuming that the installation of the PV modules is in landscape. Two configurations were studied, a south and an east-west. While a south-facing installation is optimal for energy yield per module area, a near-horizontal placement ensures best energy yield per area of structure, which takes prevalence in case of expensive structures or size limitations; a small angle is still required to ensure water run-off. For the south configuration, the inclination was set to 35° (**Figure 2b**), while for the east-west configuration, the inclination was equal to 15° and an additional PV module was mirrored on the left side (**Figure 2c**). The mesh utilized was “*Extra Fine*” and the “*Study*” applied was “*Stationary*”. In order to obtain the pressure profiles, 2D lines were cut above and below the PV module. The 2D lines were translated to 3D profiles by extending the values along the full length of the PV module. Although the 2D model is a significant simplification over the 3D model, it is sufficient enough to describe our problem, since the PV modules are assumed to be installed tightly next to each other, without leaving a gap between the two frames. Moreover, the generated pressures are similar to these obtained for a 3D model (see comparison between **Figure S2** and [14] for wind speed 20 m/s). It must be noted that the studied scenario is the worst-case, considering the PV modules that are placed on the front row of an installation [14].

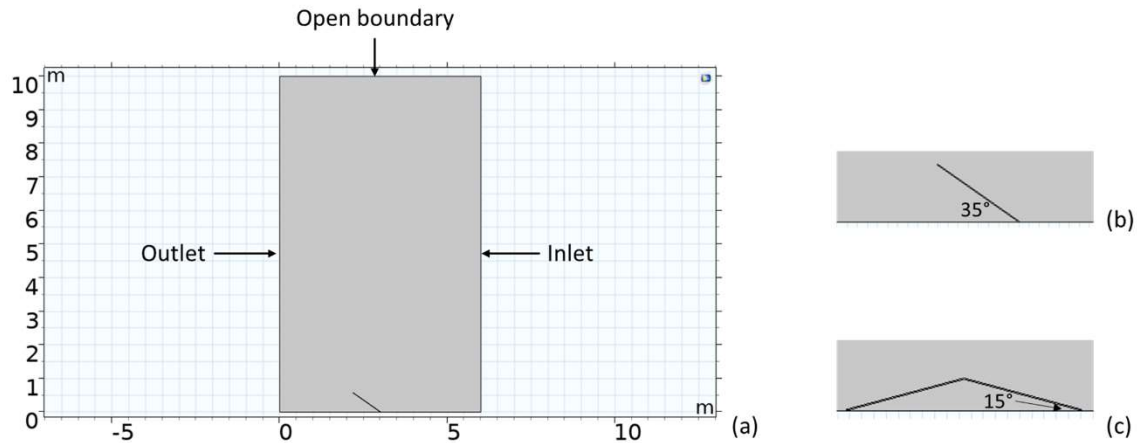


Figure 2. (a) Full geometry of the 2D wind model including boundary conditions. Specific design for (b) 35° south and (c) 15° east-west configurations.

2.2.2 First Principal Stress Maps of a PV Module – Static Mechanical Load

For the calculation of the resulting first principal stress within the PV module, the “*Solid Mechanics*” module was used. The dimensions of the simulated PV module were assumed according to the dimensions of existing PV modules in the lab, in order to achieve experimental validation (see section 2.1). In the future, modules with bigger dimensions will be examined, according to the industrial trends. As a simplification, the PV module was assumed as a layered shell including a glass – encapsulant – cells – encapsulant – glass structure. This simplification is sufficient assuming that we only investigate stationary studies (or in section 2.2.3, time dependent with very short duration) at constant temperature which do not account for the viscoelasticity of the encapsulant. Moreover, a realistic interaction between the different layers (for example defects in adhesion) is not considered since no accurate information can be found. The space between the cells was equal to 1.5 mm in both directions. The encapsulant was simulated by an Ethylene Vinyl Acetate (EVA) layer. For the weight - mechanical robustness optimization, the thickness of the glass (top and bottom simultaneously) was set to three different values 2, 2.5 and 3.2 mm. The layered shell was in continuity with the silicone edge sealant and the frame (see details in **Figure 3a** and **Figure 3b**). The main mechanical properties are listed in **Table 2**. The module was clamped (constrained regions on the rear side of the frame) at six points over its length, three on each long side (see **Figure 3c** and **Figure 3d** for the clamping locations) and not at four as in section 2.1, as the four clamps configuration was used only due to experimental limitations and six clamps would provide more reliable mechanical stability. The extracted pressure profiles for the different wind speeds, described in section 2.2.1, were applied on the front and rear side of the PV module. The effect of gravity was also considered according to the inclination. Finally, a customized mesh was generated (**Table 3**) and a “*Stationary Study*” was applied.

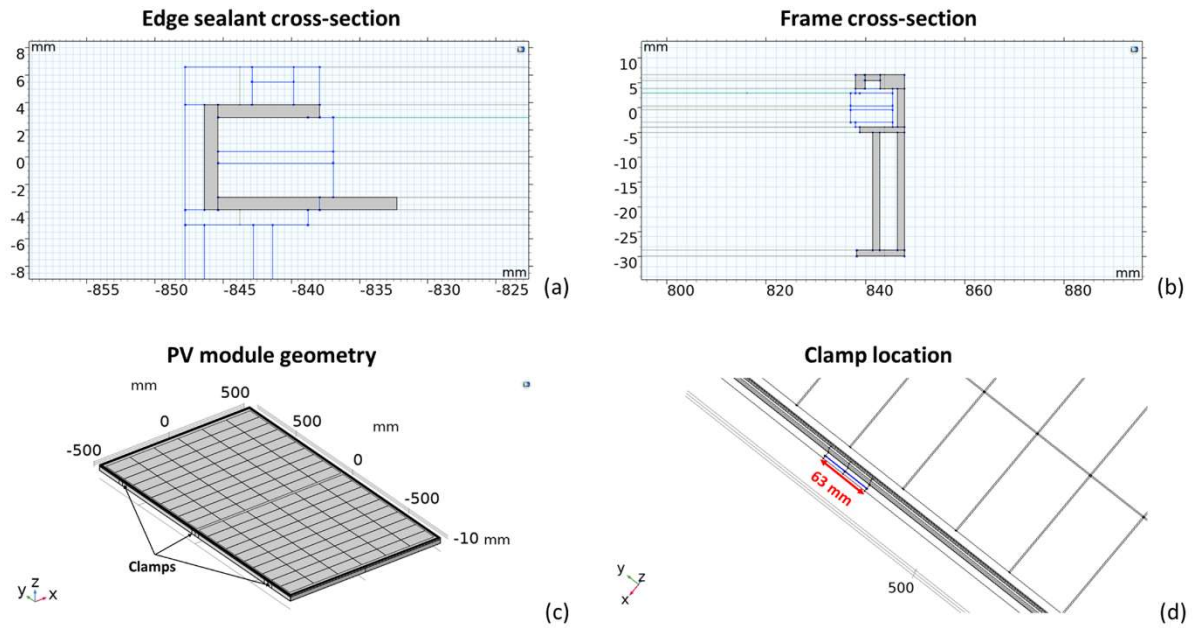


Figure 3. (a) Edge sealant and (b) frame cross-sections. (c) PV module geometry with the location of the clamps indicated. (d) Clamp location and dimensions on the rear side of the frame.

Table 2. Parameters required for the mechanical simulation of the PV modules. It must be noted that all the materials are assumed as linear elastic, as they are part of a layered shell, for simplification. Moreover, the temperature for all the simulations was considered 20 °C.

Materials	Model	Thickness (mm)	Density (kg m ⁻³)	Young's Modulus (Pa)	Poisson's Ratio
Float Glass	Linear Elastic	2-3.2	2220	$73.7 \cdot 10^9$	0.168
Silicon (cells)	Linear Elastic	0.160	2329	$170 \cdot 10^9$	0.28
EVA (encapsulant)	Linear Elastic (temperature dependent)	0.425	1760	$16.9 \cdot 10^9$	0.4995
Silicone (edge sealant)	Linear Elastic	See Figure 2a	1310	$2.1 \cdot 10^6$	0.49

Table 3. Meshing details of the PV module's geometry.

Components	Type of Mesh	Size
Glass	Free Tetrahedral	Extra fine
Cells	Free Quadrilateral	Extremely fine
Encapsulant (between the cells)	Free Triangular	Extra fine
Encapsulant (layers)	Free Tetrahedral	Extra fine
Edge-sealant	Free Tetrahedral	Extra fine
Frame	Free Tetrahedral	Extra fine

2.2.3 First Principal Stress Maps of a PV Module During the Vibration Test

For the simulation of the vibration of the PV module at the resonance frequency with the maximum acceleration (see section 2.1), an oscillation simulation was performed. The parameters described in section 2.2.2 were regarded, for a PV module with a glass thickness of 2.5 mm. Moreover, four clamps instead of six were adjusted, for replication of the experiment described in section 2.1. The center of the clamps was placed at 31 cm from the edge of the PV module (see section 2.1). A sinusoidal load was regarded with frequency 16 Hz (frequency value for the maximum recorded acceleration) and amplitude equal to the product of the mass of the PV module (26 kg) times the maximum recorded acceleration. A time dependent study was realized for time zero, $T/4$, $T/2$, $3T/4$ and T , where T was the period of the oscillation. Furthermore, a similar stationary simulation was conducted, with the sinusoidal load replaced by a uniform load of 1 kPa, for the replication of the standard DML [20] at $3T/4$.

2.2.4 Look-up Table – Translation of Wind Speed to Maximum First Principal Stress

Nine stationary simulations were carried out for wind speeds (5,10,15,...,45) m s^{-1} , according to the methodology described in section 2.2.1. By using look-up tables in MATLAB, the maximum first principal stress (MPa) and maximum deformation (mm) were determined using linear interpolation for the daily wind gust profile of Westhinder location in the North Sea (51.23°, 2.26°). The data included wind gusts in 10 min resolution for the date 10-Dec-2017 and are publicly available from Meetnet Vlaamse Banken at [21]. The wind gust values were calculated as the combined wind components and their absolute value (without taking into consideration the direction) was directly applied on the PV modules, according to the methodology described in section 2.2.2.

3. Results and Discussion

3.1 Inclination and Glass Thickness Optimization

The first optimization study considered the configuration of the arrays. **Figure 4** demonstrates the pressure distribution around a PV module, due to wind speed 45 m s^{-1} and direction from right to left (as indicated by the red arrows), and the resulting first principal stress within the PV module. We observed that a higher pressure (maximum 1.54 kPa) is applied on the front side of the PV module for the high inclination south configuration, while the low inclination east-west configuration undergoes lower pressure (maximum 0.75 kPa) (**Figure 4** top row). Regarding the translation of the pressure to first principal stress distributed within a PV module with glass thickness 2.5 mm, the highest value of stress is concentrated on the front glass near the clamps (see **Figure 4** bottom right for the location), especially the central clamp located on the lowest part (which is the left side of the PV module when it is demonstrated as a portrait configuration) of the landscape installed module (**Figure 4** bottom row), since this is where the pressure due to wind speed is the highest. The maximum first principal stress (see **Discussion S1** and **Figure S3** for the calculation procedure, which reports the mean value of a specific area where stress maxima are detected) is equal to 30.6 MPa and 14.8 MPa for the high and low inclination, respectively. The resulting first principal stress distribution over the PV module agrees with the findings of previous studies where the combination of clamps and a frame was included [14,22], confirming that the highest stress is concentrated near the clamps, but not extremely localized, since it is additionally regulated by the application of the frame. The second location of high stress is the center of the rear glass (see **Figure S3** which agrees with [14]). Additionally, it must be noted that pre-stress due to lamination is not included in our study. The glass theoretically should not break in any case, as the obtained values and their distributions (**Figure 5**) are lower than the ultimate tensile strength of the PV glass, which is $\sim 69 \text{ MPa}$ [23], although in practice, cracks might be observed in case of non-uniform tensile stress over the glass plate [24]. Moreover, a higher elastic deformation was estimated for the high inclination, equal to 4.29 mm over 2.03 mm for the low inclination.

Afterwards, three different PV glass thicknesses were considered for the 15° east-west configuration, for the weight-stress optimization. The results show that the maximum first principal stress is obtained at the same location as for the different inclinations. The maximum values, calculated as previously stated, are between 20.6 MPa and 9.8 MPa, for the thinnest (2 mm) and the thickest (3.2 mm) glass sheet, respectively. All the resulting maximum values (mean over an area where multiple stress maxima were detected) and their deviations are much lower than the ultimate tensile strength of the PV glass ($\sim 42 \text{ MPa}$ for the 2 mm glass and $\sim 69 \text{ MPa}$ for the other thicknesses) [23,25], making all the thicknesses theoretically compatible with high wind loads, according to the assumptions made for this current study.

Figure 5 represents the first principal stress at the highest stress region, for all the examined scenarios and both front and rear sides of the module. The analysis on top of the front glass shows that the 35° south installation results in higher stress than a 2 mm glass selection for a 15° east-west configuration. The same trend, but with lower values, is obtained for the bottom surface of the rear glass. Furthermore, a few outliers are present due to artifacts of the meshing near the frame. It must be noted that these values were estimated with the clamps assumed as constrained points. Different values may be obtained for different types of clamping (see **Discussion S2** and **Figure S4** for comparison with a more relaxed clamp). Moreover, the current work includes only the mechanical impact of the wind load, without accounting for the

waves occurring in a marine environment. In future work, a different type of clamping will be studied, where the modules will be clamped from an aluminum profile attached to the rear side.

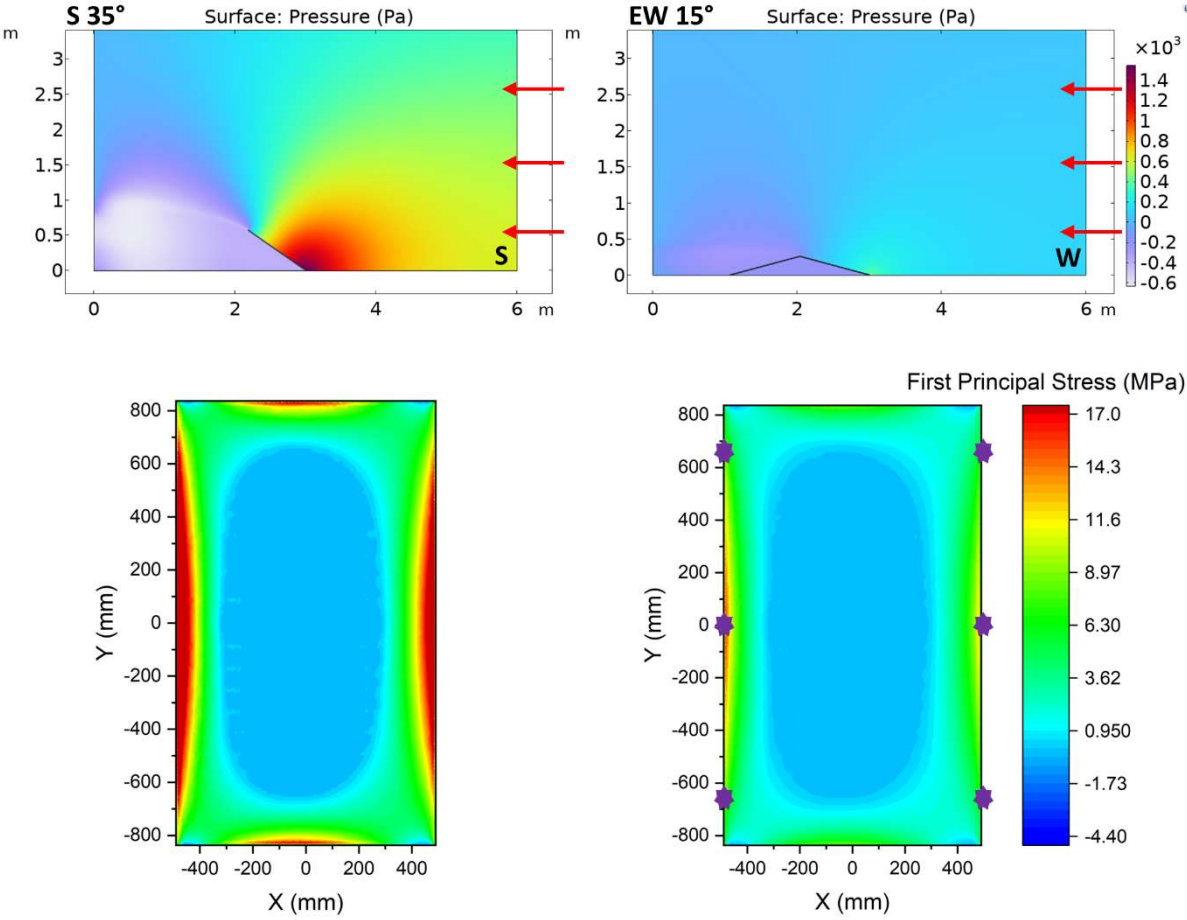


Figure 4. Pressure distribution around a PV module, due to a wind speed of 45 m s^{-1} for south (S) (top left) and east-west (EW) (top right) configuration. The red arrows indicate the direction of the wind. The respective resulting first principal stress maps for the upper surface of the top glass of an exposed PV module are presented at the bottom, left and right. The purple asterisks on the bottom right map indicate the location of the clamps. The PV module installation is landscape, meaning that the right side of the maps represents the part of the PV module which is closer to the installation platform, while the left side is the opposite.

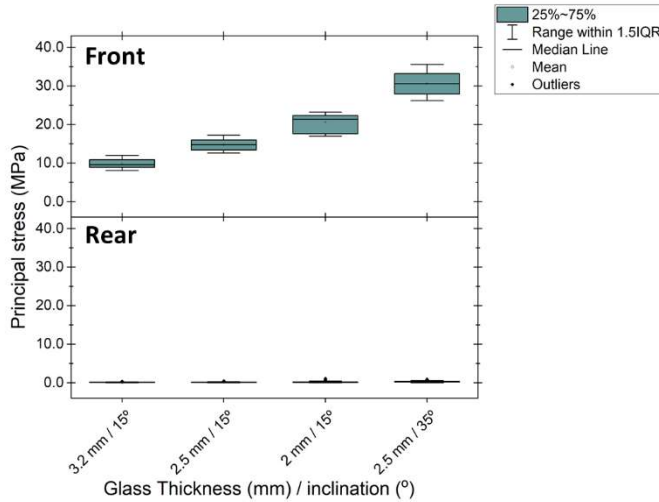


Figure 5. First principal stress at the highest stress region (near the left central clamp), for all the examined scenarios and both the front and rear sides of the PV module. The statistical analysis of the first principal stress values over a studied region is conducted according to **Discussion S1**, since the assumption of a single value may be invalid, due to meshing artifacts.

3.2 Identification of Resonance Frequencies and Internal Stress Assessment

A frequency sweep test at 1 g was conducted for the identification of the resonance frequencies of the PV module. Then the maximum acceleration and respective frequency results (highest peak in **Figure 6**) were applied to a mechanical simulation, in order to evaluate the first principal mechanical stress developed within the PV module. The combination of the frequency sweep with the accelerometer data (**Figure 6**) shows that for both tested PV modules the identified resonance frequencies are 16 Hz, 21.3 Hz and 60.7 Hz. The highest maximum deflection is observed for the 16 Hz and is equal to 15.3 mm followed by the other two mode shapes, where the maximum deformation is 5.6 mm and 0.6 mm for the second and third, respectively. An additional peak is observed below 10 Hz however, it was not analyzed due to inconsistency caused by the inadequate control of the vibration table (see section 2.1 and **Figure S1** for details). This specific peak was expected to be found according to [26]. The oscillation simulation showed maximum first principal stress of 77.3 MPa (**Figure 7**) and maximum deflection equal to 16.8 mm, which is higher than the one calculated directly from the acceleration. The maximum values for the front glass occurred at the $3T/4$ of the period T of the oscillation, as expected. Moreover, the maximum first principal stress that the module experiences is higher than the value obtained when the uniform 1 kPa load from the IEC standard DML [20] is applied (19.6 MPa), where the maximum deflection is 3.7 mm (**Figure 7**). This result was expected, since the specific acceleration applies to a PV module maximum pressure equal to ~ 2.5 kPa. Finally, although the maximum first principal stress exceeded the ultimate tensile stress of the tempered PV glass during the 16 Hz vibration, it seems that the combination of the materials of the PV laminate did not lead to glass breakage, since the ultimate tensile strength of the glass may vary when it is laminated on different materials. Another explanation may be that our simulation does not include the effect of the different interfaces between the materials, which can lead to slightly higher estimated stresses [27].

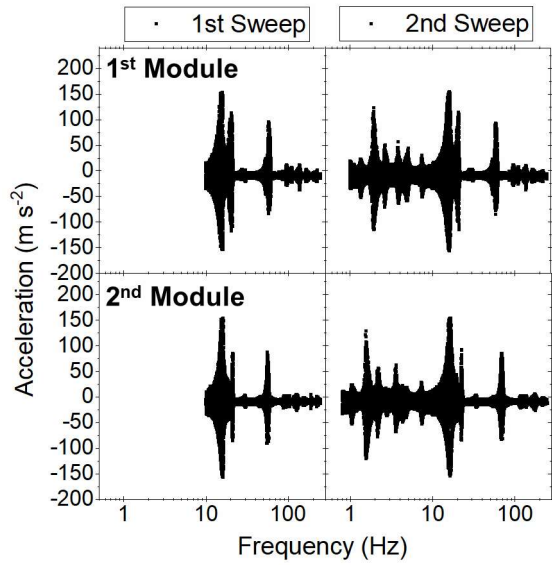


Figure 6. Acceleration measurements plotted over the frequency sweeps (1st and 2nd) for the two tested PV modules. No measurements were recorded below 10 Hz for the 1st sweep, due to inadequate control of the vibration table.

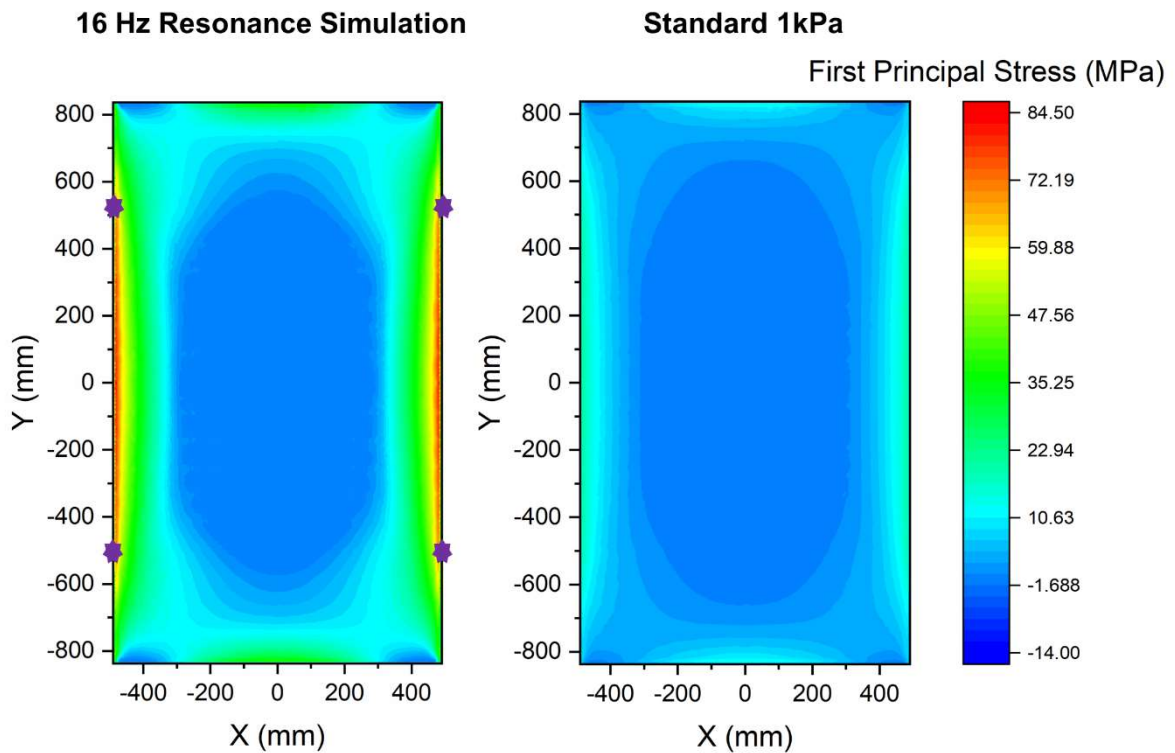


Figure 7. First principal stress map (at $3T/4$) of the upper surface of the front glass of a simulated PV module when it undergoes 16 Hz resonance at 1 g (left) and under 1 kPa uniform stationary load (right), which represents the $3T/4$ of the standard DML. For both simulations, the location of the clamps is assumed as indicated by the purple asterisks on the left side.

3.3 The Effect of Wind Speed Variation – Distinguishment Between Vibration Modes

After the generation of the look-up table, with the aim to match the responsible wind speed to maximum first principal stress and maximum deformation of a PV module, the resulting function was applied on wind gust data (absolute value of the combined components) recorded for the full day of 10-Dec-2017. The first principal stress values and deformations obtained (**Figure 8**) are indicative for one day, as certain assumptions have been made (see section 2.2.2) we do not expect modification of the PV laminate materials due to degradation. In future work, the degradation factor will be considered in the calculations. The variation of the first principal stress and deflection values is generally slow over time, leading to low vibration frequencies due to variation of wind speed. This observation remains valid for relatively high gusts of $\sim 20 \text{ m s}^{-1}$, as such gusts take almost one hour to build up. However, the vibration frequency due to variation of wind speed changes when the gusts are very strong ($\sim 45 \text{ m s}^{-1}$), but it is difficult to define it from the analyzed data, as the data are not continuous around this event, due to a low resolution (10 min). When the first principal stress values, demonstrated in **Figure 8**, are compared to these resulting from a standard DML test (see **Figure S5** for the results when 6 clamps are applied), it is concluded that the applied load 1 kPa leads to similar stresses to the stresses observed for high wind gusts [20]. For this reason, the standard DML test is not sufficient for predicting the robustness of a PV module against significantly high wind gusts, when additionally taking into consideration that, in the studied case, the inclination of the PV module is very low and the PV module is not in resonance. Higher loads such as 2.5 kPa and 5 kPa applied by [28] are more appropriate.

Additional to the vibration due to varied speed, a PV module experiences another vibration mode, when its resonance frequency is reached. In literature [15,29] it is reported that a vibration frequency of 16 Hz, which was identified also in this study and causes the highest stress to the PV module among the resonance frequencies due to the highest acceleration, can be reached during stormy weather. According to the results presented in section 3.2, this vibration may lead to more severe stress within the PV module, and it can be much more frequent, as a regular storm occurs more frequently than an extremely high wind gust. For this reason, the robustness of a module during extended vibration at the resonance frequency with the highest measured acceleration during a frequency sweep should be examined, since it is not included also in the relevant standard for transportation of PV modules [26], where the vibration frequencies are applied by a random sweep.

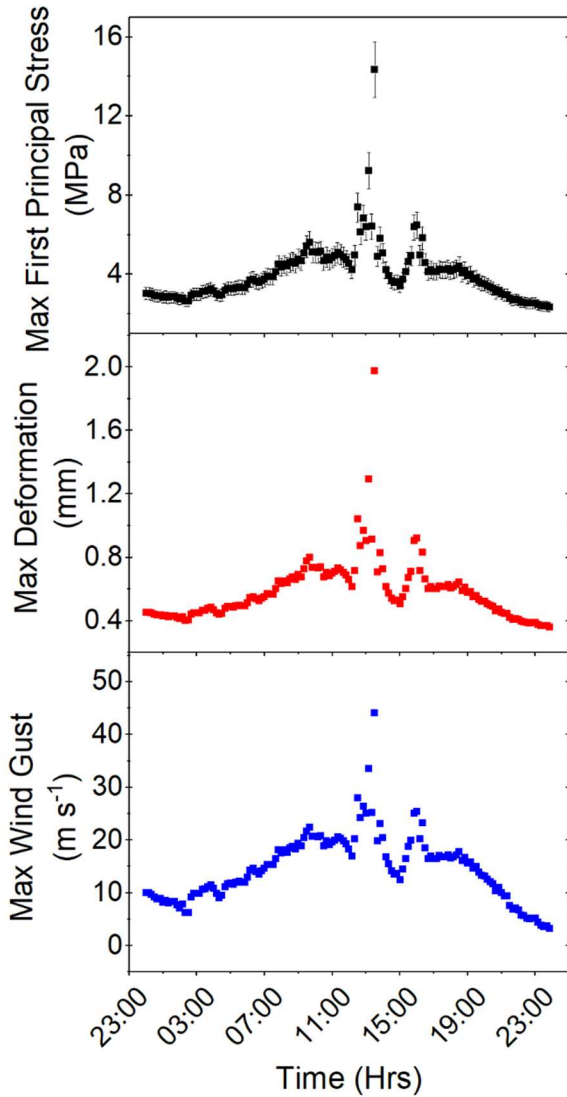


Figure 8. Wind gust data plotted simultaneously with the resulting maximum first principal stress (calculated according to **Discussion S1**) and deformation over a period of one day on 10-Dec-2017.

4. Conclusions

The purpose of the present research was to quantify the static and dynamic mechanical load due to wind gusts, when a PV module is installed offshore. Initially, the installation configuration has been varied, to evaluate the effect of the inclination on the mechanical stress. It was found that an east-west configuration with a 15° inclination reduced the first principal stress by 52% when compared to a south 35° installation. Moreover, the PV glass of 2.5 mm thickness performed adequately for both static and dynamic mechanical load. However, the long-term durability against vibration of the PV module at 16 Hz and 1g (~2.5 kPa sinusoidal) is questionable, since the maximum first principal stress exceeds the ultimate tensile strength of the tempered PV glass by 5%. Furthermore, the vibration modes due to varied wind speed and due to resonance were distinguished, with the second leading to significantly more severe first principal stress. Finally, it is highly recommended that the resonance frequencies of the PV

modules are identified and they are tested with DML at higher pressures, such as 2.5 kPa or 5 kPa, since the 1 kPa load is not enough to evaluate the r of a PV module at high wind gusts, which are more frequent and severe offshore. A longer resonance test at the frequency with the highest measured acceleration during a frequency sweep should be added, since the standard for the transportation of the PV modules includes only a random frequency sweep. In addition, the installation could be designed considering the resonance frequencies of the PV modules in order to prohibit occurrence of resonance. In future work, we will study different types of clamping, such as aluminum profiles glued on the rear side of the PV module, in order to mechanically compensate for further reduction of the glass thickness. Additionally, higher resolution of wind gust data will be analyzed, including their direction, and the degradation of the other components of a PV laminate will be studied, so their contribution is considered.

Acknowledgements

Many thanks to Materials and Packaging Research & Services and Dimitri Adons for providing the facilities and helping with the vibration test. Additionally, we would like to thank Thijs Vandenryt for his help with the accelerometer and Jan Mertens, and Geert Doumen for designing and developing the mounting configuration for the attachment of the PV module to the vibration table.

Funding Sources

This work was conducted within the project “Marine Solar POtential and Technology Study” (MarineSPOTS) project and funded under the support of the Belgian Energietransitiefonds.

Supporting Information

Supporting information cited through the paper regarding the frequency sweeps and first principal stress maps for front, rear glass and different mounting assumptions can be found in the document Kyranaki_et_al_SI_final.docx.

Generative AI in scientific writing

During the preparation of this work the authors used ChatGPT in order to improve/re-phrase some parts of the text, mainly in the introduction. After using this tool/service, the author(s) reviewed and edited the content as needed and take full responsibility for the content of the publication.

Author Contributions

Nikoleta Kyranaki: Conceptualization, Methodology, Software, Validation, Formal analysis, Investigation, Writing-Original Draft, Visualization, **Philippe Nivelles:** Methodology, Software **Sara Bouguerra:** Methodology, Software, Writing-Original Draft, **Marta Casasola Paesa:** Software, **Richard De Jong:** Software, **Oscar Delbeke:** Methodology, **Lars Spannan:** Methodology, **Arvid van der Heide:** Writing - Review & Editing, **Ismail Kaaya:** Writing - Review & Editing, **Jens D. Moschner:** Conceptualization, Methodology, Writing - Review & Editing, Project administration, **Arnaud Morlier:** Methodology, Writing - Review & Editing, Visualization, **Michaël Daenen:** Conceptualization, Methodology, Writing - Review & Editing, Supervision

References

- [1] IEA, Renewables 2023, (n.d.). <https://www.iea.org/reports/renewables-2023>.
- [2] H. Ritchie, M. Roser, P. Rosado, Renewable Energy, OurWorldInData.Org (n.d.). <https://ourworldindata.org/renewable-energy> (accessed February 27, 2024).
- [3] IEA, Solar PV, Paris, 2022. <https://www.iea.org/reports/solar-pv>.
- [4] SolarPower Europe, Solar, Biodiversity, Land Use: Best Practice Guidelines., 2022. https://api.solarpowereurope.org/uploads/4222_SPE_Biodiversity_report_03_mr_ba11900938.pdf?updated_at=2022-10-27T08%3A28%3A18.591Z (accessed February 13, 2024).
- [5] H. Liu, V. Krishna, J. Lun Leung, T. Reindl, L. Zhao, Field experience and performance analysis of floating PV technologies in the tropics, *Prog. Photovolt. Res. Appl.* 26 (2018) 957–967. <https://doi.org/10.1002/pip.3039>.
- [6] S.Z.M. Golroodbari, D.F. Vaartjes, J.B.L. Meit, A.P. Van Hoeken, M. Eberveld, H. Jonker, W.G.J.H.M. Van Sark, Pooling the cable: A techno-economic feasibility study of integrating offshore floating photovoltaic solar technology within an offshore wind park, *Sol. Energy* 219 (2021) 65–74. <https://doi.org/10.1016/j.solener.2020.12.062>.
- [7] O. Delbeke, J.D. Moschner, J. Driesen, The complementarity of offshore wind and floating photovoltaics in the Belgian North Sea, an analysis up to 2100, *Renew. Energy* 218 (2023) 119253. <https://doi.org/10.1016/j.renene.2023.119253>.
- [8] M. Kumar, H. Mohammed Niyaz, R. Gupta, Challenges and opportunities towards the development of floating photovoltaic systems, *Sol. Energy Mater. Sol. Cells* 233 (2021) 111408. <https://doi.org/10.1016/j.solmat.2021.111408>.
- [9] O.K. Segbefia, A.G. Imenes, T.O. Sætre, Moisture ingress in photovoltaic modules: A review, *Sol. Energy* 224 (2021) 889–906. <https://doi.org/10.1016/j.solener.2021.06.055>.
- [10] F. Setiawan, T. Dewi, S. Yusi, Sea Salt Deposition Effect on Output and Efficiency Losses of the Photovoltaic System; a case study in Palembang, Indonesia, *J. Phys. Conf. Ser.* 1167 (2019) 012028. <https://doi.org/10.1088/1742-6596/1167/1/012028>.
- [11] Solaredition, Destruction of Floating PV Plant by Typhoon at Yamakura Dam, Wind Resistance in Spotlight, (2020). <https://solaredition.com/destruction-of-floating-pv-plant-by-typhoon-at-yamakura-dam-wind-resistance-in-spotlight/> (accessed June 23, 2023).
- [12] T.J. Silverman, N. Bosco, M. Owen-Bellini, C. Libby, M.G. Deceglie, Millions of Small Pressure Cycles Drive Damage in Cracked Solar Cells, *IEEE J. Photovolt.* 12 (2022) 1090–1093. <https://doi.org/10.1109/JPHOTOV.2022.3177139>.
- [13] Y. Lee, A.A.O. Tay, Stress Analysis of Silicon Wafer-Based Photovoltaic Modules Under IEC 61215 Mechanical Load Test, *Energy Procedia* 33 (2013) 265–271. <https://doi.org/10.1016/j.egypro.2013.05.067>.
- [14] P. Romer, K.B. Pethani, A.J. Beinert, Effect of inhomogeneous loads on the mechanics of PV modules, *Prog. Photovolt. Res. Appl.* 32 (2024) 84–101. <https://doi.org/10.1002/pip.3738>.
- [15] M. Assmus, S. Jack, K.-A. Weiss, M. Koehl, Measurement and simulation of vibrations of PV-modules induced by dynamic mechanical loads: Measurement and simulation of vibrations of PV-modules, *Prog. Photovolt. Res. Appl.* 19 (2011) 688–694. <https://doi.org/10.1002/pip.1087>.
- [16] A. Kilikevičius, A. Čereška, K. Kilikevičienė, Analysis of external dynamic loads influence to photovoltaic module structural performance, *Eng. Fail. Anal.* 66 (2016) 445–454. <https://doi.org/10.1016/j.engfailanal.2016.04.031>.
- [17] J. Estephan, A. Gan Chowdhury, P. Irwin, A new experimental-numerical approach to estimate peak wind loads on roof-mounted photovoltaic systems by incorporating inflow turbulence and dynamic effects, *Eng. Struct.* 252 (2022) 113739. <https://doi.org/10.1016/j.engstruct.2021.113739>.

- [18] B.L. Allsopp, R. Orman, S.R. Johnson, I. Baistow, G. Sanderson, P. Sundberg, C. Stålhandske, L. Grund, A. Andersson, J. Booth, P.A. Bingham, S. Karlsson, Towards improved cover glasses for photovoltaic devices, *Prog. Photovolt. Res. Appl.* 28 (2020) 1187–1206. <https://doi.org/10.1002/pip.3334>.
- [19] W. Frei, Which Turbulence Model Should I Choose for My CFD Application?, *Comsol Blog* (n.d.). <https://www.comsol.com/blogs/which-turbulence-model-should-choose-cfd-application> (accessed July 2, 2024).
- [20] IEC TS 62782:2016 Photovoltaic (PV) modules - Cyclic (dynamic) mechanical load testing, (n.d.). <https://webstore.iec.ch/publication/24310> (accessed July 11, 2023).
- [21] Vlaanderen, AGENTSCHAP MARITIEME DIENSTVERLENING EN KUST, (n.d.). <https://meetnetvlaamsebanken.be/Measurement> (accessed July 14, 2023).
- [22] J. Dong, H. Yang, X. Lu, H. Zhang, J. Peng, Comparative Study on Static and Dynamic Analyses of an Ultra-thin Double-Glazing PV Module Based on FEM, *Energy Procedia* 75 (2015) 343–348. <https://doi.org/10.1016/j.egypro.2015.07.382>.
- [23] NY Engineers, Tempered Glass: Properties and Applications, (n.d.). <https://www.ny-engineers.com/blog/tempered-glass-properties-and-applications> (accessed January 30, 2023).
- [24] K.B. Doyle, M.A. Kahan, Design strength of optical glass, in: A.E. Hatheway (Ed.), *San Diego, California, USA, 2003*: p. 14. <https://doi.org/10.1117/12.506610>.
- [25] Xinology, Ultra Clear Glass for Photovoltaic Solar Panel, (n.d.). <http://www.xinology.com/Glass-Mirrors-Products/solar-glass/specifications.html> (accessed January 29, 2023).
- [26] IEC 62759-1:2022 Photovoltaic (PV) modules - Transportation testing - Part 1: Transportation and shipping of module package units, (n.d.). <https://webstore.iec.ch/publication/64172> (accessed February 13, 2024).
- [27] S.-H. Schulze, M. Pander, K. Naumenko, H. Altenbach, Analysis of laminated glass beams for photovoltaic applications, *Int. J. Solids Struct.* 49 (2012) 2027–2036. <https://doi.org/10.1016/j.ijsolstr.2012.03.028>.
- [28] Sinovoltaics, Dynamic Mechanical Load Testing, (n.d.). <https://sinovoltaics.com/dynamic-mechanical-load-testing/> (accessed July 13, 2023).
- [29] H. Xu, K. Ding, G. Shen, H. Du, Y. Chen, Experimental investigation on wind-induced vibration of photovoltaic modules supported by suspension cables, *Eng. Struct.* 299 (2024) 117125. <https://doi.org/10.1016/j.engstruct.2023.117125>.